Clays valorization as corrosion inhibitors for E400 reinforcing steel

Diadioly GASSAMA,[1] Modou FALL,[2,*] Ismaïla YADE,[2] Serigne Massamba SECK,[2] Mababa DIAGNE[3] and Mouhamadou Bassir DIOP[3]

[1]*UFR Sciences & Technologies, Université de Thiès, Thiès, Sénégal*
[2]*Laboratoire de Chimie Physique Organique et d'Analyses Environnementales, Département de Chimie, Faculté des Sciences et Techniques, Université Cheikh Anta Diop, Dakar, Sénégal*
[3]*Institut des Sciences de la Terre (IST), BP 5396, Faculté des Sciences et Techniques, Université Cheikh Anta Diop, Dakar, Sénégal*

Abstract. The behavior of E400 steel, a constructional steel widely used in Senegal, was studied in aqueous NaCl solution in the presence of two types of clay: volcanic tuffs, and sedimentary montmorillonite. The protection efficiency of these compounds were electrochemically assessed (corrosion potential variation curves, polarization curves and electrochemical impedance spectroscopy) at various inhibitor contents. The results obtained showed that these inhibitors present an inhibitory efficacy of about 70% for an optimal concentration of 0.60% for the tuffs and 62% for a maximum content of 0.50% for montmorillonite.

Keywords: corrosion; inhibitor; steel; tuffs; montmorillonite; Tafel polarization.

1. Introduction

Steels are alloys used in mechanical engineering and are necessary in most technical application fields. They are characterized by good resistance to general corrosion, which is not the case as regards localized corrosions. The corrosion of a metal in aqueous media results from the oxidation of the metal, sometimes because of the oxygen dissolved in water [1], but also because of aggressive ions present in the corrosive media. Corrosion is an electrochemical process and no approach related to it can be carried out within the framework of an electrochemical representation of the involved processes [2]. Although electrochemistry laws are the same for all materials, their practical efficiency is somewhat different and very often depends on their chemical composition and the environment.

Aqueous corrosion is studied by electrochemical means, whereas dry corrosion is often analyzed through physical measurements which are performed periodically on samples exposed for a long time [3-7]. Only few research concerning the kinetic survey in initial atmosphere corrosion is available in literature [8].

The use of reinforcing steel as building material in bridges, buildings and other structures is nowadays of paramount importance, and the problem of corrosion is still persistent. Several studies revealed the existence of a variety of oxoanions, for example chromates, nitrites, etc., identified as inhibitors of steel

corrosion in aqueous environments [9]. In neutral media, the inhibitor reaction is linked to oxygen and requires its presence in such media. There is a lower risk of attack if oxygen is prevented from appearing on the surface (cathode inhibition). Alternately, by passivating the metal the reaction rate can be slowed down (anodic inhibition) [10, 11]. By reasons of the toxicity of most commonly used oxoanions, finding more environment-friendly compounds is necessary for researchers. Thus, organic inhibitors based on sodium benzoate and other aromatic substituted acid salts and fatty acids have been proposed by Kuznetsov *et al.* [12-15]. Most of these inhibitors have proved to be effective from a "critical minimum concentration" [16]. More recently, some minerals are more and more used as steel corrosion inhibitors. These are different classes of clay used as nanocomposites incorporated in coatings [17-18]. Other studies were focused on iron corrosion in an aqueous medium filled with clay bricks [19], steel pipelines in clayey soils ore [20] or zinc corrosion inhibition by a clay mineral exchanger ore [21]. In our previous works [22-23] we examined the impact of chloride ions on the corrosion rate of E400 [22] and S275, S235 and S435 steels [23]. The materials were exposed to a simulated marine atmosphere produced by an aqueous solution of 0.5 M NaCl. In the case of E400 steel, we noticed that after 15 days, nearly the total surface was attacked. These studies showed that exposure of E400 steel to simulated marine atmosphere (near marine zones, for

---

* Corresponding author: modou.fall@ucad.edu.sn

example) not only modified the corrosion level but also the kinetics of the reaction in relation to the results obtained during an exposure in a non-saline atmosphere. We also reported preliminary works dealing with the study of E400 corrosion inhibition by tuffs [22].

In this work, we examine the corrosion behavior of E400 steel in the absence and in the presence of two types of natural clay: tuffs (volcanic clay products) collected at Bafoundou, Eastern Senegal and montmorillonite (a clayey sediment) of the region of Dakar, Senegal. The aim is to establish the capacity of selected clays to provide effective corrosion inhibition of E400 building material and to compare, in the same conditions, their relative efficiencies.

2. Experimental

The electrochemical measurements were carried out on samples taken from E400 steel bars of 10 mm diameter and 12 m long with the following centesimal chemical composition: C : 0.24%; P : 0.055%; N : 0.013 and Fe (balance), provided by Pôle de Développement Industriel (PDI), Dakar, Senegal. The samples are in the form of cylinders, cut into washers by a universal pair of shears Gruchoir, then coated in "Epoxy Steel" type resins. The washer surface in contact with the solution is 0.785 cm^2. Before each test, the working electrode was abraded with abrasive paper of varying size (600; 800; 1000 and 1200 µm), then rinsed with distilled water and dried in the open air.

Electrochemical measurements were performed using a three-electrode assembly: a platinum wire serving as the counter electrode, Ag/AgCl electrode (+197 mV/NHE) as the reference and the sample, acting as the working electrode. The measurements were performed using a µAutolab type III + FRA2 potentiostat - galvanostat (Eco Chemie, Netherlands) driven by GPES (General Purpose for Electrochemical System) or FRA (Frequency Response Analyzer), enabling the working electrode polarization. The Tafel method, a quantitative technique that allows for a fast determination of some mechanistic insights and an

estimation of corrosion rates, was employed in this work. The Tafel method consists of polarizing the electrode in the Tafel zone (we chose to work in the domain $E_{corr} \pm 250$ mV), then in fitting the experimental values into the theoretical model of Stern-Geary [24]. The scanning speed was set to 0.5 mV/s and the equilibrium time to 1800 seconds. Beforehand the working electrode is kept in immersion at the free corrosion potential for an hour under magnetic agitation. The electrochemical parameters (i_{corr}, E_{corr}, R_p, b_a and b_c) were determined from the Tafel polarization curves in relation to the Stern- Geary equation after ohmic drop compensation.

The inhibitory efficacy was calculated from the following formula [25]:

$$IE = \frac{i_{corr}^0 - i_{corr}}{i_{corr}^0} \times 100 \qquad (1)$$

i_{corr}^0 and i_{corr} represent the corrosion current densities without and with an inhibitor, respectively.

Electrochemical impedance spectroscopy (EIS) measurements were made on the steel samples by applying 5 mV AC on the open circuit potential at frequencies ranging from 10 kHz to 0.1 Hz, with 5 points/decade. Before running any EIS measurement, the working electrode was held at its open-circuit potential for an equilibrium time of 30 min to obtain a steady state. Both electrochemical techniques were repeated twice on each sample and the average value was reported. The inhibitory efficacy was evaluated according to Eq. (2) [25].

$$IE = \frac{R_P - R_P^0}{R_P} \times 100 \qquad (2)$$

R_P^0 and R_P represent charge transfer resistances, without and with an inhibitor, respectively.

We evaluated the inhibitory potency of the Bafoundou tuffs and montmorillonite. Their chemical compositions are given in Table 1. Other characteristics such as crystallographic, mechanical and morphological properties are available in literature [26, 27].

Table 1. Chemical composition of the clays (wt-%) [26, 27].

Compound	SiO$_2$	Al$_2$O$_3$	Fe$_2$O$_3$	CaO	MgO	K$_2$O	Na$_2$O	TiO$_2$	Mn$_2$O$_3$	H$_2$O	P$_2$O$_5$	LOI	Reactive silica
Tuffs	69.7	13.3	10.1	0.1	0.1	1.3	0.6	0.8	0.1	-	0.03	4	8.9
Montmorillonite	58.6	20.4	3.4	-	1.9	0.2	3.1	0.3	-	12	-	-	-

3. Results and Discussions

3.1. Open-circuit potentials

The evolution of the free-corrosion potential (or open-circuit potential) during a corrosion study is a first clue to estimate the eventual severity of the degradation of the metal. The sample was immersed in the solution and the evolution of the working electrode

free-corrosion potential with time was recorded. Figure 1 shows the evolution of the free-corrosion potential during 2 hours of immersion at room temperature in 0.5 M aqueous NaCl solution, at different inhibitors concentrations.

The results are given in Table 2. They showed clearly the effect of the inhibitor concentration on the corrosion potential. We noted a cathodic shift of the

free-corrosion potential when the inhibitors were added, indicating that the clays act as cathodic inhibitors. The free-corrosion potential decreased first with the inhibitor content, reached a minimum at 0.50% (montmorillonite) and 0.60% (tuffs) and then increased. This tendency may be attributable to the inhibitor action which results in the formation of a protective film layer from a given percentage in the solution, thus reducing the corrosion rate.
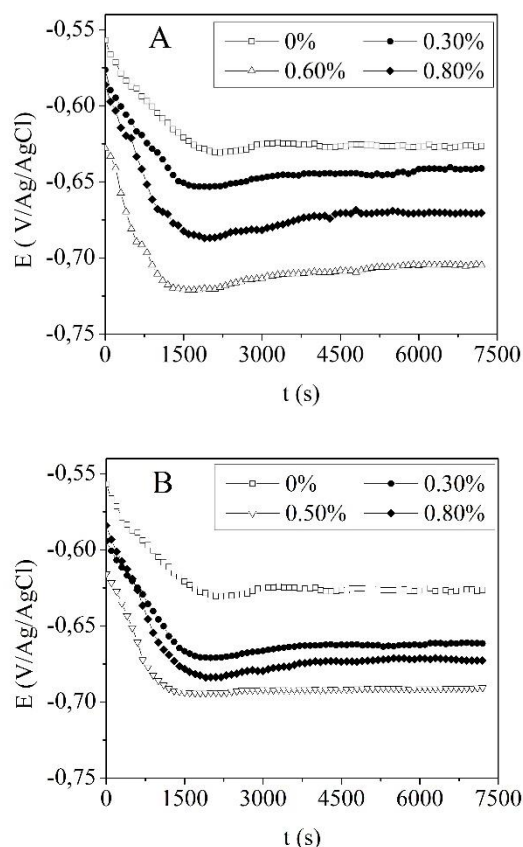
Table 2. Free-corrosion potential E_{corr} (V/Ag/AgCl) measured for E400 steel in 0.5 M NaCl.

Clay (%)	Tuffs		Montmorillonite	
	E_{corr}	ΔE(mV)	E_{corr}	ΔE(mV)
0	-625	0	-625	0
0.20	-632	-7	-650	-25
0.30	-642	-17	-661	-36
0.40	-658	-33	-676	-51
0.50	-671	-46	-692	-67
0.60	-705	-80	-682	-57
0.70	-678	-53	-664	-39
0.80	-669	-44	-672	-47

3.2. Polarization curves

Stationary polarization curves of E400 steel spotted after two hours of immersion, with and without inhibitors under agitation are represented in Fig. 2. A study of this figure shows that the addition of an inhibitor brings about a significant reduction in the corrosion current for concentrations below 0.60% (tuffs) and 0.50% (montmorillonite), by comparison with a medium without inhibitor and an important shift of the corrosion potentials towards cathodic values. Beyond the optimal contents, corrosion current densities and potential increase.
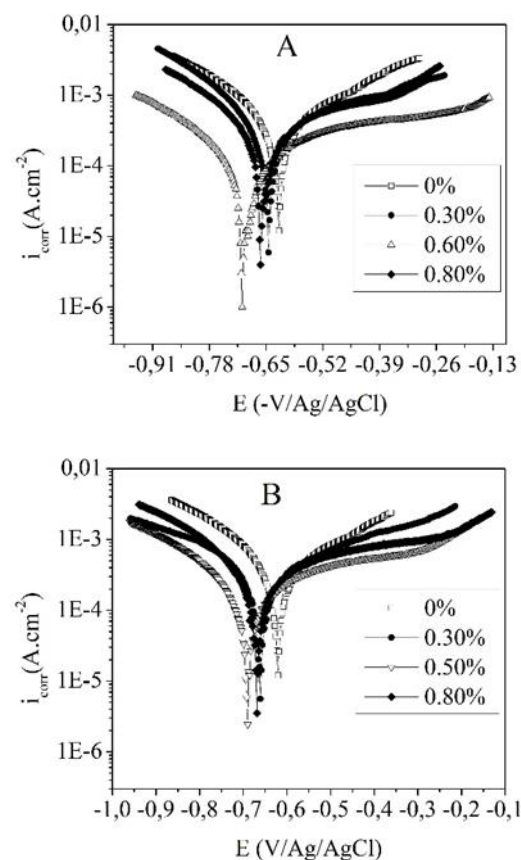

Figure 1. Temporal evolution of E400 steel corrosion potential in 0.5 M NaCl solution. A: Bafoundou tuffs; B: montmorillonite.

As shown by the ΔE (difference between the free-corrosion potential in the presence and in the absence of inhibitor) values, the shift was more pronounced in the case of montmorillonite, for clay contents ranging from 0.1% to 0.5%. Beyond that value, the trend is reversed because the maximal content is reached for montmorillonite, but not for the tuffs. In that range of concentrations, montmorillonite appeared therefore to be more efficient than the tuffs.

For all the curves, it appeared that the free-corrosion potential (E_{corr}) tended to stabilize at around 1500 seconds of immersion. Therefore, we chose an equilibrium time of 30 min for the polarization measurements.

Figure 2. Stationary polarization curves of E400 steel in salt water (0.5 M NaCl). (A): Bafoundou tuffs; (B): montmorillonite.

To clearly point out the effect of the added inhibitors on the corrosion kinetics, we represented in Table 3 the collected current densities in the anodic domain (E = -0.450 V/Ag/AgCl) and in the cathode domain (E = -0,850 V/Ag/AgCl) for all tested rates.

Table 3 shows first a decrease in current densities up to the clay optimal content, and a slight increase afterwards. For a potential of -0.850 V/Ag/AgCl, the values of the current densities in the presence of an inhibitor are between 2550 and 469 µA·cm^{-2} for the Bafoundou tuffs and between 2476 and 762 µA·cm^{-2} for montmorillonite whereas in the absence of an inhibitor the value is 3275 µA·cm^{-2}. Similarly, for -0.450 V/Ag/AgCl, i_{corr} values range from 1025 to 388 µA·cm^{-2} for the tuffs and from 1095 to 426 µA·cm^{-2} for

montmorillonite whereas in the absence of an inhibitor the value is 1164 µA·cm^{-2}.

Up to a clay content of 0.5%, the current densities are lower for montmorillonite compared to the tuffs. This confirms that montmorillonite should be more efficient than the tuffs from 0.1 to 0.5%.

We noticed that in the presence of inhibitor, anodic and cathodic current densities decrease and reach a minimum at about 0.60% and 0.50% for tuffs and montmorillonite, respectively. Moreover, the corrosion potential values are slightly displaced to less noble values.

In the anodic domain, there is probably a change of the steel corrosion mechanism in the corrosive solution in the presence of an inhibitor.

Table 3. Current density (in µA·cm^{-2}) for a potential of -0,850 V/Ag/AgCl (cathodic domain) and -0.450 V/Ag/AgCl (anodic domain) for the different inhibitor contents: A: Bafoundou tuffs; B: Montmorillonite.

		0%	0.20%	0.30%	0.40%	0.50%	0.60%	0.70%	0.80%
A	-0.850 V/Ag/AgCl	3275	2550	2693	1527	1498	469	865	1886
	-0.450 V/Ag/AgCl	1164	1025	733	610	583	388	526	819
B	0.850 V/Ag/AgCl	3275	2476	1247	954	762	959	1433	1658
	-0.450 V/Ag/AgCl	1164	1095	972	545	426	524	564	712

In fact, we noted a decrease of the current density in comparison with an environment without inhibitor for all the concentrations below 0.60% (tuffs) and 0.50% (Montmorillonite). We also remarked the appearance of a current plateau in a wide potential range (of about 400 mV) in the vicinity of the optimum content (0.50 - 0.60%) for both clays. However the length of the current plateau decreases as the inhibitory content decreases. We noted that at equal concentrations the length of the inhibitor plateau of Bafoundou tuffs is still greater than that of montmorillonite. The presence of this plateau can be explained by the formation of an inhibitory film with protective properties on the metal surface [28]. Beyond that, the value of the current density increases more rapidly. This can be due to the occurrence of a localized corrosion or a removal of the inhibitory film from the metal, which increases the active surface. If it is only a partial blocking, this can lead to an increase of the current density on the surface and then to a generalized corrosion process, more intense than in the absence of an inhibitor according to the importance of the content in active elements. As far as weak anodic potentials are concerned, the anodic current density slightly increases with overvoltage. When the desorption potential (*E*d) or (non-polarizability) [29-31] is exceeded, clays virtually have no effect on anodic curves, the anodic current density swiftly increases and the metal is dissolved with a steeper slope in the area of high potentials. The abrupt increase of the anodic current density after the desorption potential is attributable to desorption of clay molecules adsorbed at the steel surface, which shows clearly that the mode of inhibition of this compound depends on

the electrode potential. The nature of the observed protection can be described as being the result of an inhibitor layer adsorbed at the electrode surface [32].

We also noticed that the values of the desorption potential are nearly constant (about -600 mV/Ag/AgCl) for the different contents in tuffs. This leads us to believe that the values of the desorption potential of clays are slightly modified by the recovery of the inhibitor molecules. This result is accepted in literature [33]. Nevertheless, beyond the optimum inhibitor content, we noticed an increase of the corrosion rate. This phenomenon may be due to the formation of deposits of insoluble corrosion products. On account of the local changes, the damage mechanisms can evolve together with the corrosion phenomenon [34]. This continuous corrosion beyond the optimal clay concentration leads to a new displacement of the potential towards anodic values.

The Tafel cathodic slopes variations in the absence and in the presence of the inhibitor show that the oxidation reaction at the steel surface is not modified by adding the clays. The inhibitor is first adsorbed onto the surface steel by simply blocking its active sites. The cathodic inhibitors induce an increase of cathode overvoltage and reduce the corrosion current.

Though these inhibitors do not totally stop the corrosion reaction, they do not constitute a danger in localized corrosion.

The electrochemical parameters drawn from these curves are given in Table 4. The corrosion current densities and the polarization resistances vary in opposite directions, but a maximum (resistance) or a minimum (current density) at 0.60% (tuffs) or 0.50% (montmorillonite). The inhibitory potency increased

with the concentration of substances and reached a maximum value of 69.7% for a content of 0.60% as regards tuffs.

For montmorillonite we have a maximum value of 61.4% but for a lower clay content (0.50 %). These

inhibitory efficiencies are satisfactory as it appears that the corrosion rate could be cut by about 70% by adding only 0.60% of tuffs, or by about 61% with only 0.50% of montmorillonite.

Table 4. Electrochemical parameters resulting from intensity-potential curves of E 400 steel in salt water (0.5 M NaCl) at different concentrations of inhibitors.

	c (%)	E_{corr} (mV/Ag/AgCl)	i_{corr} (µA cm^{-2})	R_p (Ω.cm^2)	b_c (mV/dec)	b_a (mV/dec)	V_{corr} (mm/year)	$E\%$
Bafoundou tuffs	0	-621	318.2	37.0	174	203	7.45	-
	0.20	-638	288.0	40.7	160	151	6.76	9.5
	0.30	-645	264.6	44.4	151	196	6.22	16.8
	0.40	-657	195.1	60.1	197	225	4.58	38.7
	0.50	-673	149.0	78.7	135	201	3.50	53.2
	0.60	-706	96.3	125.7	133	264	2.26	69.7
	0.70	-688	137.4	85.3	157	257	3.23	56.8
	0.80	-663	175.9	66.5	141	204	4.13	44.7
Montmorillonite	0	-621	318.2	37.0	174	203	7.45	-
	0.20	-647	285.4	41.1	172	227	6.72	10.3
	0.30	-661	254.4	46.1	168	225	5.98	20.0
	0.40	-673	159.6	74.5	167	232	3.68	49.8
	0.50	-690	122.7	93.9	131	276	2.90	61.4
	0.60	-681	132.3	87.9	147	248	3.15	58.4
	0.70	-675	160.3	74.0	148	263	3.71	49.6
	0.80	-669	196.1	60.1	154	207	4.63	38.4

3.3. Electrochemical impedance spectroscopy

We also studied E400 material corrosion by EIS in the presence and in the absence of the two clays. Figure 3 represents the electrochemical impedance diagrams in the Nyquist plan of E400 steel in 0.5 M NaCl aqueous solution at various inhibitors proportion.

The graphs were recorded after immersion during 2 hours at room temperature (25±2°C) at the open-circuit potential and in the frequency range of 100 kHz-100 mHz. The impedance diagrams show the appearance quasi flat loops with a significant increase of the polarization resistance. At high frequencies the size of the capacitive loop increases with the concentration. This is attributed to the formation of an inhibitor film with a barrier effect against the aggressive ions [35]. At low frequencies, the addition of inhibitors lead to an increase in the charge-transfer resistance (R_{ct}) value (diameter of the loop between high and low frequency) which has a non-monotonous variation in relation to the inhibitor content. The highest value is obtained for a concentration of 0.60% (130 Ω·cm^2) for the Bafoundou tuffs and 0.50% (105 Ω·cm^2) for montmorillonite (Table 5). This can be attributable to charge transfer from the solution to the metal [36]. To characterize the steel / solution interface, we have used the modified Randles equivalent circuit shown in Fig. 4, where R_s and R_{ct} designate the solution and charge transfer resistances,

and the double layer capacitance simulated here as a constant phase element (CPE). A CPE is a component that models the behavior of a double layer that is an imperfect capacitor.

Table 5 shows that the transfer resistance increases up to the optimal concentration value (0.60%) and then decreases gradually as the inhibitor content increases. The reduction of dissolved oxygen may occur at the metal surface. However, inhibition in neutral medium seems to be complex, because of the reaction of iron with oxygen and water which can give rise to more corrosion products (various iron hydroxides) and also complicate the adsorption process.

Corrosion inhibitors which increase the ohmic resistance of the electrolyte are considered in some cases, as filming inhibitors (anode and cathode).

The solution resistance increases due to the formation of a film on the metal surface [37]. The difference between R_s values in the presence and in the absence of inhibitors is attributed to that film.

The variations of the inhibitory efficacy of these substances with their concentrations are plotted in Fig. 5. The values obtained by polarization and EIS methods are very close. We note that there exist for both inhibitors an optimal content for which the inhibitory efficacy reaches a maximum: 69.7% in the presence of tuffs while for montmorillonite it is 62.3%. These values are in accordance with those obtained with the Tafel polarization curves (69.7% and 61.4%, respectively).
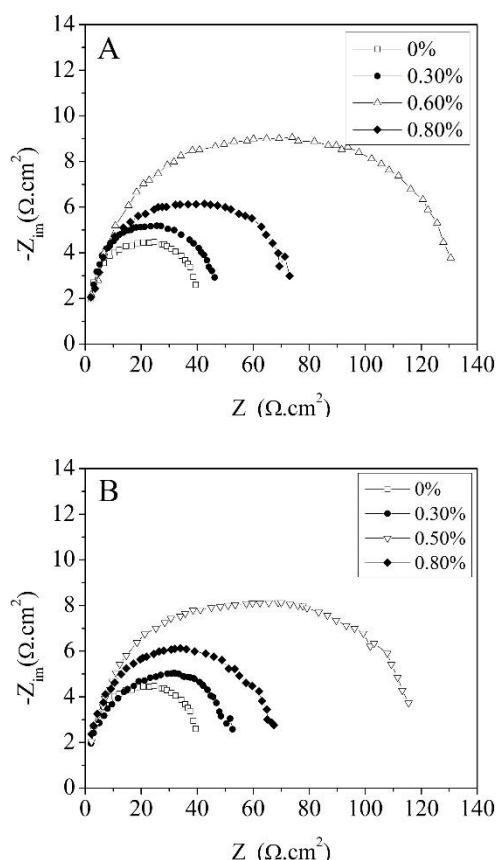
Figure 3. Electrochemical impedance diagrams of E400 steel in 0.5 M aqueous NaCl solution. (A): tuffs; (B): montmorillonite.

The protection is effective at an optimal content of 0.50-0.60%. Beyond, tuffs are more efficient than montmorillonite. This is in accordance with results obtained by Yuan *et al.* [38]. In a recent work, these authors found that corrosion resistance of hot-dip galvanized (HDG) steels in sodium silicate (mixture of

SiO_2 and Na_2O) was increased by the SiO_2/Na_2O molar ratio. From the compositions given in Table 1, the SiO_2/Na_2O molar ratio is higher for tuffs compared to montmorillonite.
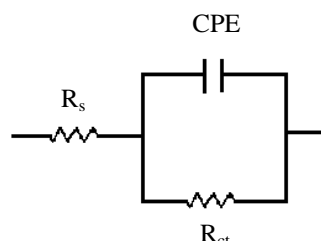

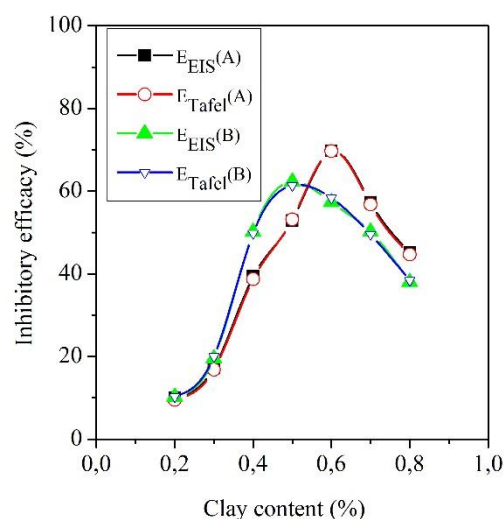**Figure 4.** Electrical equivalent circuit for the modeling of the impedance spectra.

Figure 5. Variation of the inhibitory efficacy with the inhibitor content. A: tuffs; B: montmorillonite.

Table 5. EIS results at open-circuit potential for E400 steel 0.5 M aqueous NaCl at different inhibitors concentration.

	c (%)	R_s ($\Omega \cdot cm^2$)	R_{ct} ($\Omega \cdot cm^2$)	CPE ($\mu F \cdot cm^{-2}$)	n	C ($\mu F \cdot cm^{-2}$)	τ (s)	$E\%$ (SIE)	$E\%$ (Tafel)
Bafoundou Tuffs	0	2.6	39.5	284.8	0.87	1147.6	0.045	-	-
	0.20	3.0	43.8	246.2	0.86	1116.5	0.049	10.0	9.5
	0.30	3.0	47.7	244.8	0.83	1666.4	0.079	17.2	16.8
	0.40	3.4	65.0	187.7	0.85	987.7	0.064	39.3	38.7
	0.50	3.5	83.7	140.6	0.84	838.2	0.070	52.9	53.2
	0.60	3.6	130.0	134.1	0.86	657.5	0.085	69.7	69.7
	0.70	3.4	92.4	171.2	0.81	1654.0	0.153	57.3	56.8
	0.80	3.3	71.9	185.3	0.84	1131.2	0.081	45.2	44.7
Montmorillonite	0	2.6	39.5	284.8	0.87	1147.6	0.045	-	-
	0.20	2.9	43.9	232.4	0.80	2336.1	0.103	10.2	10.3
	0.30	3.0	49.0	228.9	0.85	1186.7	0.058	19.5	20.0
	0.40	3.0	79.1	166.1	0.85	885.5	0.070	50.1	49.8
	0.50	3.3	104.5	176.4	0.81	1766.5	0.185	62.3	61.4

c (%)	R_s (Ω·cm²)	R_{ct} (Ω·cm²)	CPE (µF·cm⁻²)	n	C (µF·cm⁻²)	τ (s)	E% (SIE)	E% (Tafel)
0.60	3.3	93.4	143.6	0.91	367.6	0.034	57.3	58.4
0.70	3.1	79.2	160.9	0.86	749.6	0.059	50.2	49.6
0.80	3.1	63.6	177.7	0.82	1378.6	0.088	38.0	38.4

We can calculate and compare the time constants once the pure capacitances (*C*) are known. These can be obtained from the CPE (*Q*) and the charge-transfer resistance using the following equation [36, 37, 39]:

$$Q = R^{n-1}C^n \qquad \text{(Eq.3)}$$

The CPE becomes capacity when the constant phase coefficient (*n*) is equal to 1.

The time constant (*τ*) can then be obtained using the equation below [36, 37, 39]:

$$\tau = RC \qquad \text{(Eq.4)}$$

The time constant calculation results are given in Table 5. We obtain quite similar values for both inhibitors. They are comprised between 0.04 and 0.18 seconds, indicating that the equivalent electrical circuit is associated with a slow charge/discharge process [36, 39,40].

4. Conclusions

The E400 steel aqueous corrosion inhibition by natural clays was studied in a simulated sea-water for a protection of installations against corrosion. A protection by a 70% reduction of the corrosion rate of ordinary E400 steel has been achieved by using these ecological inhibitors: the Bafoundou tuffs and montmorillonite, which acted as cathodic inhibitors. The results are promising as the corrosion of E400 material which is used in civil engineering could be reduced by about 70% by adding only 0.60% of tuffs, and by 62% with a maximum content of 0.50% for montmorillonite.

References

[1] T.W. Swaddle, *An Industrial and Environmental Perspective; Corrosion of Metals*, Academic Press, San Diego, **1997**, 327.

[2] S. Krakowiak, K. Darowicki, P. Slepski, *Electrochimica Acta* **50**, 2699 (2005).

[3] T. Nishimura, H. Katayama, K. Noda, T. Kodama, *Corrosion Science* **42**, 1611 (2000).

[4] S. Hoerlé, F. Mazaudier, P, Dillmann, G. Santarini, *Corrosion Science* **46**, 1431 (2004).

[5] Y.Y. Chen, H.J. Tzeng, L.I. Wei, L.H. Wang, J.C. Oung, H.C. Shih, *Corrosion Science* **47**, 1001 (2005).

[6] M. Natesan, G. Venkatachari, N. Palaniswamy, *Corrosion Science* **48**, 3584 (2006).

[7] E. Burger, M. Fénart, S. Perrin, D. Neff, P. Dillmann, *Corrosion Science* **53**, 2122 (2011).

[8] J.P. Cai, S.B. Lyon, *Corrosion Science* **47**, 2956 (2005).

[9] P. Agarwal, D.Landolt, Corrosion Science, **40**, 673 (1998).

[10] G. Trabenelli, *Corrosion Mechanisms*, Marcel Dekker, NY, **1987**, 119.

[11] D. Landolt, *Traité des Matériaux. Vol. 12: Corrosion et Chimie de Surface des Métaux*, Presses Polytechniques Universitaires Romandes, Lausanne, **1997**, 492.

[12] Y.I. Kuznetsov, *Organic Inhibitors of Corrosion of Metals*, Plenum Press, NY, **1996**.

[13] Y.I. Kuznetsov, N.N. Andreev, *Zastchita Metallov* **23**, 495, (1987).

[14] Y.I. Kuznetsov, *Zastchita Metallov* **26**, 954 (1990).

[15] N.N. Andreev, S.V. Lapshina, Y.I. Kuznetsov, *Zastchita Metallov* **28**, 1017 (1992).

[16] G. Reinhard, M. Radtke, U. Rammelt, *Corrosion Science* **33**, 307 (1992).

[17] A.H. Navarchian, M. Joulazadeh, F. Karimi, *Progress in Organic Coat*ings **77**, 347 (2014).

[18] C. Motte, M. Poelman, A. Roobroeck, M. Fedel, F. Deflorian, M. G. Olivier, *Progress in Organic Coatings* **74**, 326 (2012).

[19] F.A. Martin, C. Bataillon, M.L. Schlegel, *Journal of Nuclear Mat*erials **379**, 80 (2008).

[20] M. Yan, C. Sun, J. Xu, J. Dong, W. Ke, *Corrosion Science* **80**, 309 (2014).

[21] A. Aït Aghzzaf, B. Rhouta, E. Rocca, A. Khalil, J. Steinmetz, *Corrosion Science* **80**, 46 (2014).

[22] D. Gassama, S.M. Seck, I. Yade, M. Fall, M.B. Diop, *Journal de la Société Ouest-Africaine de Chimie* **38**, 64 (2014).

[23] D. Gassama, A.A. Diagne, I. Yade, M. Fall, S. Faty, *Bulletin of the Chemical Society of Ethiopia* **29**, 299 (2015).

[24] M. Stern, A.L. Geary, *Journal of Electrochemical Society* **104**, 56 (1957).

[25] M. Doubi, A. Dermaj, H. Ramli, D. Chebabe, N. Hajjaji, A. Srhir, *ScienceLib Editions Mersenne* **5,** 130110 (2013).

[26] M.B. Diop, M.W. Grutzeck, *Construction and Building Materials* **22,** 114 (2008).

[27] L.K. Boudalia, A. Ghorbela, H. Amrid, F. Figueras, *Compte Rendus Académie des Sciences, Paris, Série IIc, Chimie/Chemistry* **6,** 7 (2001).

[28] W.J. Lorentz, F. Mansfeld, *Electrochimica Acta* **31,** 467 (1986).

[29] F. Bentiss, M. Bouanis, B. Mernari, M. Traisnel, M. Lagrenee, *Journal of Applied Electrochemistry* **32**, 671 (2002).

[30] K.E. Heusler, G.H. Cartledge, *Journal of Electrochemical Society* **108,** 732 (1961).

[31] M. Bartos, N. Hackerman, *Journal of Electrochemical Society* **139,** 3428 (1992).

[32] Y. Feng, K.S. Siow, W.K. Teo, A.K. Hsieh, *Corrosion Science* **41,** 829 (1999).

[33] N. Srisuwan, N. Ochoa, N. Pebere, B. Tribollet, *Corrosion Science* **50,** 1245 (2008).

[34] J.L. Crolet, in *Corrosion localisée,* Ed. F. Dabosi et al., Les Editions de Physique, Les Ulis, (1994), p. 407.

[35] R. Touir, N. Dkhireche, M. Ebn Touhami, M. Sfaira, O. Senhaji, J.J. Robind, B. Boutevin and M. Cherkaoui, *Materials Chemistry and Physics* **122,** 1 (2010).

[36] A. Belloufi, Mémoire de Magister, Université de Batna, 2010.

[37] I. Danaee, K.M. Niknejad, A.A. Attar, *Journal of Materials Science and Technology* **29,** 89 (2013).

[38] M. Yuan, J. Lu, G. Kong, *Surface Coatings Technology* **204***,* 1229 (2010).

[39] S. S. Tamil, V. Raman, N. Rajendran, *Journal of Applied Electrochemistry* **33,** 1175 (2003).

[40] M. Outirite, M. Lagrenée, M. Lebrini, M. Traisnel, C. Jama, H. Vezin, F. Bentiss, *Electrochimica Acta* **55,** 1670 (2010).